USING Δ^{95}Mo TO TRACE LATE CARBONACEOUS AND NON-CARBONACEOUS CONTRIBUTIONS TO THE EARTH AND MARS.

R. A. Fischer[1], F. Nimmo[2], and T. Kleine[3], [1]Harvard University, [2]University of California Santa Cruz, [3]University of Münster.

Introduction: Understanding the building blocks of the Earth and other terrestrial planets has important implications for the process of accretion in our Solar System; the delivery of more volatile-rich material to these planets, which may relate to the origins of life; and the initial distributions of volatile-rich material and redox gradients in the disk. To probe the later stages of accretion, it is useful to look to more siderophile elements [e.g., 1–3], since earlier-accreted siderophile elements are predominantly sequestered into the planet's core during core formation. Here we use Mo isotopes to investigate the later stages of accretion on Earth and Mars.

A recent study [4] noted that all carbonaceous-type (CC) meteorites plot on a straight line in ε^{95}Mo– ε^{94}Mo space, while all non-carbonaceous-type (NC) meteorites plot on a different, parallel line, with both of these trends parallel to an s-process mixing line (Figure 1). The Bulk Silicate Earth (BSE) falls intermediate between these two trends (Figure 1). Δ^{95}Mo quantifies the distance between these data and the s-process mixing line passing through the origin; as such, Δ^{95}Mo provides unique isotopic signatures of distinct early disk reservoirs [4]. The CC trendline exhibits Δ^{95}Mo = +26 ± 2, the NC trendline exhibits Δ^{95}Mo = –9 ± 2, and the BSE has Δ^{95}Mo = +7 ± 5 [4]. This result indicates that 46 ± 15% of the BSE's Mo was from carbonaceous precursors [4], with the remainder coming from non-carbonaceous precursors. The BSE's Mo is thought to reflect the last ~12% of Earth's accreted material [5].

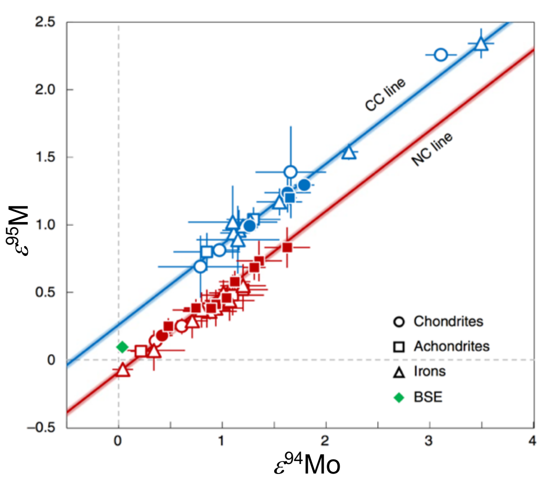

Figure 1. Previous results on the Mo isotopic compositions of CC and NC meteorites and the BSE [from 4].

In this study, we have modeled the accumulation of Mo in the mantles of Earth and Mars and their isotopic compositions. We use *N*-body simulations of terrestrial planet accretion to describe the mass evolution and provenance of Earth and Mars. Assuming an inner disk of initially NC composition and outer disk of initially CC composition, we investigate where the NC/CC divide would have to be to reproduce the observed BSE composition in various accretion scenarios, and then use the model to predict the Δ^{95}Mo of the Martian mantle.

Methods: A suite of 100 *N*-body simulations of terrestrial planet accretion was used [6], with Jupiter and Saturn on either their modern-day, slightly eccentric orbits (Eccentric Jupiter and Saturn, or EJS), or on more circular orbits, as predicted by the Nice model (Circular Jupiter and Saturn, or CJS). A suite of 16 *N*-body simulations run in the Grand Tack scenario were also used for preliminary calculations [7]. Earth and Mars analogues were identified from the planets that formed in these simulations based on their masses and semimajor axes. The accumulation of Mo in planetary mantles was defined as a cumulative distribution function $CDF(x) = x^{\kappa+1}$, where $\kappa = \frac{D*CMF*k}{1-CMF}$, *D* is the metal–silicate partition coefficient of Mo, *CMF* is core mass fraction, *k* is the fraction of accreted metal that participates in metal–silicate equilibration, and *x* is the mass fraction of the planet accreted [5]. κ is nominally 24 for Mo in Earth [5]; different values for κ will be explored for Mars, though it is likely similar due to a lower *D* [e.g., 8] and higher *k* [e.g., 9]. The Mo isotopic composition of planetary mantles was tracked using a mass balance.

Results for Earth: The average Δ^{95}Mo for Earth analogues was tracked in various accretion scenarios for different NC/CC divide locations (Figure 2a).

EJS. To match the observed Δ^{95}Mo of the BSE, the EJS case requires an initial NC/CC divide at 1.2–1.7 AU (Figure 2a). This may be unrealistic, as the preservation of the NC/CC dichotomy requires a physical barrier between reservoirs. It is not clear what dynamically could cause a barrier to arise at this location/time in the disk.

CJS. The CJS case requires an initial NC/CC divide farther out in the disk, at 1.8–2.5 AU (Figure 2a). This range of locations (especially the upper end of this range) may be consistent with the idea that CC material originates from beyond Jupiter's orbit [10–11] and was scattered inward by Jupiter's growth [12].

Grand Tack. Calculations in the Grand Tack case are ongoing, but the required NC/CC divide location can be evaluated qualitatively. A planet's mass-weighted semimajor axis can be calculated as $MWSMA = \frac{\sum_i m_i a_i}{\sum_i m_i}$, where m_i and a_i are the mass and semimajor axis, respectively, of each accreted body i. In the CJS case, late accreted material to the Earth has a MWSMA of 2.0 ± 0.3 AU, while in the Grand Tack case, it has a MWSMA of 1.7 ± 0.1 AU [13]. This implies that Earth analogues formed in the Grand Tack case should contain more late NC material than in the CJS case, and should therefore require an NC/CC divide that is closer to the Sun than in the CJS case to reproduce the Earth's observed composition. This location is likely inconsistent with Jupiter's location, which is thought to be the cause of the NC/CC divide in the Grand Tack case [e.g., 14].

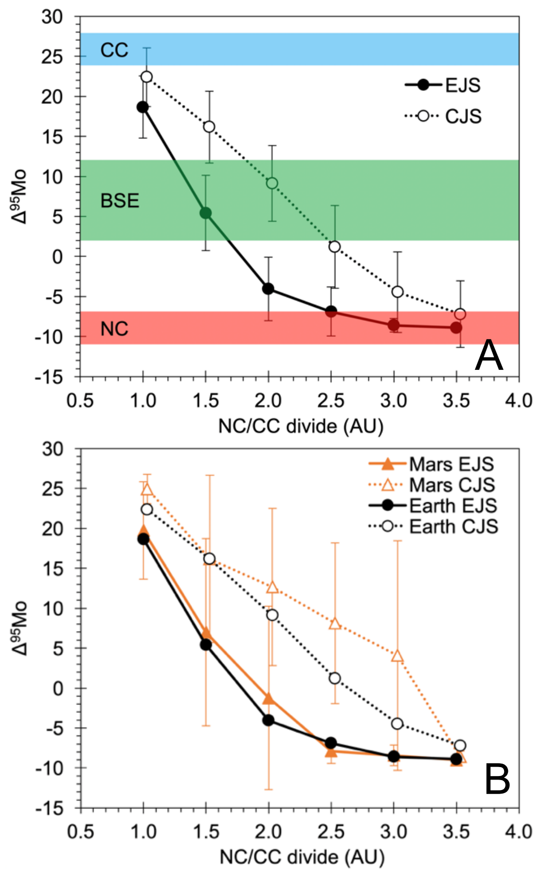

Figure 2. A: Mo isotopic compositions of Earth analogues, compared to the observed Δ^{95}Mo of CC and NC endmembers and the BSE [4]. B: Mo isotopic compositions of Mars analogues compared to Earth analogues.

Sensitivity to parameters used. We tested different values of κ (corresponding to different D or k), which affects how late in Earth's accretion history the mantle starts accumulating Mo. We found that the Earth's Δ^{95}Mo is fairly insensitive to this parameter, which caused a maximum of ±2 in Δ^{95}Mo for realistic variations in D and k, much less than the variability due to stochastic variations in accretion (error bars, Figure 2).

Results for Mars: For both EJS and CJS cases, the Δ^{95}Mo of Mars analogues are fairly similar to those of Earth analogues, or perhaps slightly higher, especially in the CJS case (Figure 2b), which is a testable prediction of our model. Our calculations for Mars analogues have larger uncertainties than for Earth analogues, both because fewer Mars analogues form in these simulations [6] and because they have much lower masses than Earth analogues, making them more subject to stochastic variations in accretion. For NC/CC divide locations that provide a match to the Earth's composition, Mars analogues have a composition that is intermediate between the CC and NC endmembers. This result implies that last ~12% of accreted material to Mars, like that on Earth, was a ~50:50 mixture of CC and NC material.

Conclusions and Future Work: In the EJS scenario, Earth's isotopic composition implies an NC/CC divide that may be too close to the Sun to be realistic. In the CJS case, the NC/CC divide should be at 1.8–2.5 AU, which may be consistent with CC material being scattered inward by Jupiter's growth [12]. Preliminarily, the Grand Tack case seems to require an NC/CC divide closer to the Sun than in the CJS case, which may be inconsistent with Jupiter's location. In the EJS and CJS cases, Mars analogues have a Δ^{95}Mo value intermediate between NC and CC, and similar to or slightly higher than Earth's, implying that the last ~12% of accreted material to Mars was a mixture of NC and CC.

We are currently undertaking more detailed calculations in the Grand Tack case, and working on incorporating Mo into a more complex core formation model [15]. In the future, this methodology could be combined with isotopes of other elements, such as oxygen stable isotopes or the Hf–W system [16].

References: [1] Walker R. J. et al. (2015) *Chem. Geol.*, *411*, 125–142. [2] Dauphas N. et al. (2014) *Phil. Trans. R. Soc. A*, *372*, 20130244. [3] Brandon A. D. et al. (2012) *GCA*, *76*, 206–235. [4] Budde G. et al. (2019) *Nat. Astron.*, *3*, 736–741. [5] Dauphas N. (2017) *Nature*, *541*, 521–524. [6] Fischer R. A. and Ciesla F. J. (2014) *EPSL*, *392*, 28–38. [7] O'Brien D. P. et al. (2014) *Icarus*, *239*, 74–84. [8] Righter K. and Chabot N. L. (2011) *MAPS*, *46*, 157–176. [9] Brennan M. C. et al. (2020) *EPSL*, *530*, 115923. [10] Warren P. H. (2011) *EPSL*, *311*, 93–100. [11] Kruijer T. S. et al. (2017) *PNAS*, *114*, 6712–6716. [12] Raymond S. N. and Izidoro A. (2017) *Icarus*, *297*, 134–148. [13] Fischer R. A. et al. (2018) *EPSL*, *482*, 105–114. [14] Morbidelli A. et al. (2016) *Icarus*, *267*, 368–376. [15] Fischer R. A. et al. (2017) *EPSL*, *458*, 252–262. [16] Fischer R. A. and Nimmo F. (2018) *EPSL*, *499*, 257–265.